Ultrafast Nonlinear Response of Bulk Plasmons in Highly Doped ZnO Layers

Tobias Tyborski,[1] Sascha Kalusniak,[2] Sergey Sadofev,[2] Fritz Henneberger,[2,*] Michael Woerner,[1,†] and Thomas Elsaesser[1]
[1]*Max-Born-Institut für Nichtlineare Optik und Kurzzeitspektroskopie, D-12489 Berlin, Germany*
[2]*Institut für Physik, Humboldt-Universität zu Berlin, D-12489 Berlin, Germany*
(Received 19 May 2015; published 28 September 2015)

Longitudinal bulk plasmons in an *n*-doped ZnO layer system are studied by two-color femtosecond pump-probe spectroscopy in the midinfrared. The optical bulk plasmon resonance identified in linear reflectivity spectra undergoes a strong redshift and a limited broadening upon intraband excitation of electrons. The nonlinear changes of plasmon absorption decay on a time scale of 2 ps and originate from the intraband redistribution of electrons. Theoretical calculations explain the plasmon redshift by the transient increase of the ensemble-averaged electron mass and the concomitantly reduced plasma frequency in the hot electron plasma. The observed bulk plasmon nonlinearity holds strong potential for applications in plasmonics.

DOI: 10.1103/PhysRevLett.115.147401 PACS numbers: 78.47.J-, 42.50.Md, 71.45.Gm, 73.21.Ac

Plasmons are elementary excitations of solids in which a plasma of free electrons undergoes a collective motion relative to the polar or ionic crystal lattice [1]. The plasma frequency $\omega_p = \sqrt{N_e e^2/(m_{\text{eff}}\epsilon_0)}$ contains the electron density N_e and the effective mass of electrons m_{eff}, the latter being determined by the electronic band structure of the material. The excitation energy $\hbar\omega_p$ covers a range from approximately 100 meV in moderately *n*-doped semiconductors to more than 10 eV in metals such as Al or Be.

In a broad range of physics, the interaction of plasmons with electromagnetic radiation has received strong interest [2,3]. The related research field of "plasmonics" aims at implementing new linear and nonlinear optical properties in tailored (meta)materials [4] and at optically probing elementary excitations on a subwavelength scale with the help of metallic nanostructures [5,6]. Such work mainly exploits surface plasmon polaritons (SPPs), which represent a coupled plasma-light excitation confined to the skin depth with electric field components essentially parallel to the surface. Wave vector conservation in optical excitation of SPPs requires a sufficient in-plane light field, as has been generated in total-reflection geometries [7] and/or with the help of grating structures at the surface [8,9]. Recently, epitaxially grown, highly *n*-doped ZnO has been introduced as a plasmonic material that allows for preparing atomically sharp interfaces between different layers at different electron concentrations [10,11]. Variation of the layer sequence and thickness as well as the doping level has allowed for tailoring SPP and/or metal-metal interface polariton (MMIP) [12] dispersion relations in wide range.

In contrast to SPPs and MMIPs, bulk plasmons represent a longitudinal excitation with an electric field perpendicular to the surface. As a result, bulk plasmons cannot couple to a transversal light field. They have mainly been studied by electron loss spectroscopy [13] while work on their optical properties has remained scarce [14]. The novel *n*-doped ZnO system allows for tailoring layer thicknesses well below the skin depth. Under such conditions, one polariton branch becomes more "bulklike" with a pronounced electric field component perpendicular to the surface [15]. Such "bulk" plasmons should interact with an optical field oriented along the same direction. In this way, the linear and nonlinear optical properties of bulk plasmons and their so far unexplored ultrafast nonequilibrium dynamics become accessible. In this Letter, we present the first ultrafast optical study of bulk plasmons in highly *n*-doped semiconductors. Using a layered ZnO system, we determine linear optical properties and apply femtosecond pump-probe spectroscopy to map the dynamics of bulk plasmons. We demonstrate transient shifts of the plasma frequency on a 300 fs time scale and a reshaping of the plasmon absorption profile persisting for several picoseconds. The strong polar electron-phonon coupling in ZnO results in a transient optical-phonon sideband of plasmon absorption during the temporal overlap of pump and probe pulses.

The sample studied in our experiments was grown by molecular beam epitaxy and consists of two Ga-doped ZnO layers grown on a sapphire substrate [Fig. 1(a)]. The 100 nm thick top layer has a doping concentration of $N_e = 1.0 \times 10^{20}$ cm^{-3} while the 400 nm thick layer underneath contains an electron density of $N_e = 6.0 \times 10^{20}$ cm^{-3}. Linear reflectivity spectra of the sample were measured in an infrared spectrometer with *p*-polarized light under angles of incidence of 45 deg and 54 deg [Fig. 1(b)]. The incoming beam traverses the top layer of the sample and is reflected from the highly doped bottom layer. The superposition of the incoming and reflected beam results in an electric field component normal to the sample surface which interacts with the bulk plasmon in the top layer. In contrast to SPPs, the position of the plasmon resonance is independent from the angle of incidence.

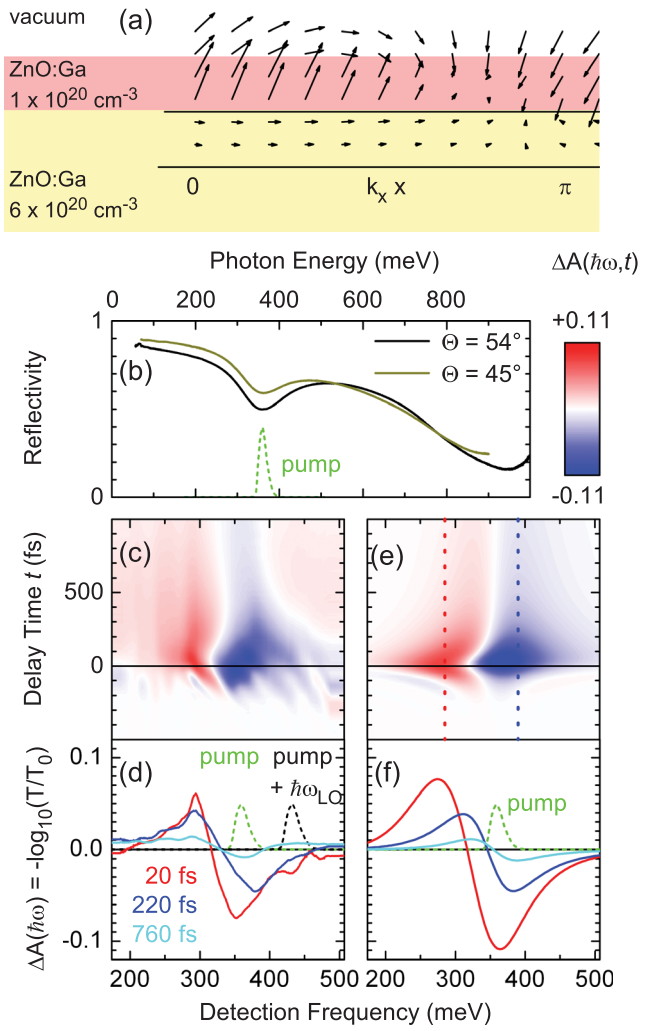

FIG. 1 (color). (a) Interaction geometry of p-polarized light with the Ga-doped ZnO layer structure. The electron density in the 100 nm thick top layer has a value of $N_e = 1.0 \times 10^{20}$ cm^{-3} while the "metallic" 400 nm thick bottom layer has a value of $N_e = 6.0 \times 10^{20}$ cm^{-3}. The small arrows represent the electric field distribution as calculated from the Fresnel equations. (b) Linear reflectivity of the sample measured for angles of incidence of 45 deg and 54 deg. The resonance at 360 meV originates from the bulk plasmon of the top layer. The green dashed line is the pump spectrum in the femtosecond experiments. (c) Contour plot of the femtosecond pump-probe data. The change of absorbance ΔA is plotted as a function of probe energy (abscissa) and pump-probe delay (ordinate). (d) Cross sections through the contour plot for fixed delay times. At early delay times, one observes a LO phonon sideband up-shifted by approximately 70 meV. (e),(f) Contour plot and spectral cuts of the calculated transient spectra.

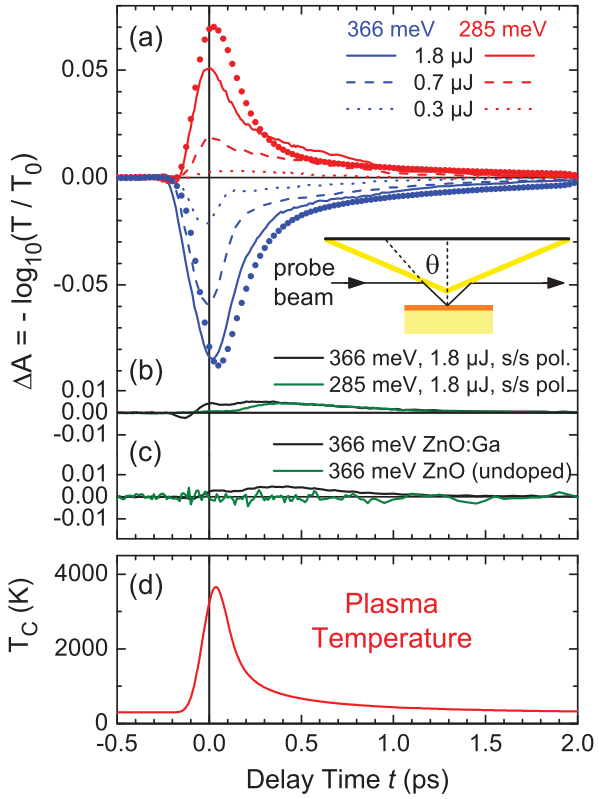

FIG. 2 (color). Time-resolved absorption changes for the measured ZnO:Ga plasmon and reference samples at fixed probe frequencies plotted as a function of pump-probe delay. (a) Measured transients of plasmon absorption for different incident pump fluences with p/p polarization (lines). Symbols represent plasmon kinetics calculated from the theoretical model for an incident pump fluence of 1.8 μJ and convoluted with the finite duration of the probe pulse. The inset shows the measurement geometry based on a Au-coated prism. The slightly noncollinear pump beam (not shown) is also reflected at the prism and spatially overlapped with the probe beam at the sample. (b) Measured transients with s/s pump and probe polarizations. (c) Measured transients from a ZnO:Ga monolayer ($N_e = 6 \times 10^{20}$ cm^{-3}, 400 nm thick) and an undoped ZnO epilayer, p/p polarization. (d) Calculated plasma temperature as a function of the delay time.

The spectra in Fig. 1(b) display a transmission decrease around $\hbar\omega \approx 1$ eV that is caused by the plasma edge of the highly doped bottom layer. The well-separated feature around $\hbar\omega_p = 360$ meV represents the bulk plasmon resonance. This fact is confirmed by calculations of the electric field distribution [vector pattern in Fig. 1(a)] with the help of the Fresnel equations. Fresnel equations are applicable here since the Thomas-Fermi screening length in the top layer $\lambda_{TF} \approx 6 \times 10^{-10}$ m is much smaller than its thickness. The vector plot shows that p-polarized light couples directly to the bulk plasmon in the thin layer, whereas the much lower electric field in the bottom layer underneath is oriented parallel to the interface; i.e., the highly doped layer acts essentially as a "metallic" mirror. In the femtosecond pump-probe experiments, the interaction geometry shown in the inset of Fig. 2(a) was applied. The incoming p-polarized infrared pulse is reflected from the front facet of a Au-coated prism under an angle close to 45 deg. The beam then enters the layered sample, traverses the upper layer, and is reflected from the highly doped second layer. The reflected beam passes the top layer again

and is reflected at the exit facet of the prism. Slightly different angles of incidence of pump and probe beams are chosen to spatially separate them after passing the second prism facet. The pump-induced change of absorbance $\Delta A = -\log_{10}(T/T_0)$ of the probe is measured as a function of pump-probe delay (T and T_0 represent transmission with and without excitation). The transmitted probe pulses were spectrally dispersed and detected by a 64-pixel HgCdTe array detector (resolution 1 meV). To cover the very wide spectral range from 180 to 500 meV, spectra were measured with probe pulses at 16 different center frequencies, and the different partial spectra were combined according to

$$\Delta A(\hbar\omega_{\mathrm{det}}, t) = \frac{\sum_{n=1}^{16} \Delta A_n(\hbar\omega_{\mathrm{det}}, t) I_n^{\mathrm{probe}}(\hbar\omega_{\mathrm{det}})}{\sum_{n=1}^{16} I_n^{\mathrm{probe}}(\hbar\omega_{\mathrm{det}})}. \quad (1)$$

$\Delta A_n(\hbar\omega_{\mathrm{det}}, t)$ and $I_n^{\mathrm{probe}}(\hbar\omega_{\mathrm{det}})$ are the transient spectrum measured with and the transmitted spectral density of the probe pulse (spectral width $\Delta\hbar\omega_{\mathrm{probe}} \approx 40$ meV), respectively [16]. p-polarized pump and probe pulses independently tunable in the midinfrared were generated in two parametric frequency converters [17] driven by a femtosecond Ti:sapphire laser system (repetition rate 1 kHz, pulse duration < 50 fs). The cross-correlation of the two midinfrared pulses has a typical width of 150 fs (FWHM). 30% of the incident pump pulse energy of 1.8 μJ are absorbed by the sample (focal diameter 150 μm). The energy of the probe pulses was less than 50 nJ.

Spectrally resolved pump-probe data are presented in Figs. 1(c) and 1(d). Figure 1(c) shows a contour plot [cf. Eq. (1)] of $\Delta A(\hbar\omega_{\mathrm{det}}, t)$ as a function of $\hbar\omega_{\mathrm{det}}$ (abscissa) and delay time t (ordinate). Cross sections of the contour plot for different fixed delay times are plotted in Fig. 1(d). At $t = 20$ fs, we observe a broad bleaching signal with a maximum around 350 meV and a redshifted enhanced absorption with a maximum at 290 meV. Upon redshifting, the overall oscillator strength is somewhat reduced. During the temporal pump-probe overlap, we find an additional bleaching peak for probe frequencies which are separated by the LO phonon energy of 70 meV [18] [black dashed line in Fig. 1(d)] from the pump pulse (green dashed line). This feature points to a pronounced interaction of the plasmon in the thin ZnO layer with LO phonons, mediated by the strong polar-optical coupling in ZnO. A similar spectral feature has been observed on intersubband transitions of electrons in GaN-based heterostructures [19].

The main signature of the transient spectra in the time range $0 < t < 400$ fs, the dispersive spectral envelope, indicates a distinct redshift of the plasmon resonance. The amplitude of ΔA reaches high values of up to 0.08, most pronounced in the bleaching region. This behavior is consistent with a transient decrease of the plasma frequency by about 50 meV and a reduced oscillator strength. Time-resolved transients of the absorption change recorded at fixed probe frequencies are summarized in Fig. 2(a) (lines). All transients rise within the time resolution of the experiment; i.e., there is no perturbed free-induction decay at negative delay times. With increasing pump fluence, the signal amplitudes begin to saturate. The enhanced absorption and bleaching components display a similar time evolution with an initial partial fast decay, followed by a slower time evolution with decay times of the order of 500 fs. The absorption changes vanish completely beyond a 2 ps delay.

The bulk plasmon character of the observed nonlinear response is validated by reference measurements with pump and probe pulses of out-of-plane (s) polarization, i.e., without a longitudinal electric field component. Under such conditions, much smaller solely positive absorption changes of about 0.005 [Fig. 2(b)] occur over the complete spectral range while signatures of plasmonic absorption are absent. A similar behavior was observed with an n-doped ZnO monolayer [Fig. 2(c), $N_e = 6 \times 10^{20}$ cm^{-3}]. An undoped ZnO layer exhibits a significantly smaller linear reflectivity and does not show any pump-induced response [Fig. 2(c)]. We conclude that the predominant nonlinear response shown in Figs. 1(c), 1(d), and 2(a) stems from the bulk plasmon in the top ZnO layer.

We now discuss the physical mechanisms determining the nonlinear bulk plasmon response. Since the layer thicknesses in our sample are much larger than the (Thomas-Fermi) screening length, the linear optical properties of the plasmon are adequately described by the frequency-dependent longitudinal dielectric function:

$$\epsilon_c(\omega) = \epsilon_\infty^c - \frac{2e_0^2}{V} \sum_{\vec{k}} \frac{f(\vec{k})}{m_{\mathrm{eff}}^c(\vec{k})[\omega^2 + i\omega\gamma_m(\vec{k})]}. \quad (2)$$

This expression is based on the Boltzmann transport equation for intraband transitions within the conduction band of the material. The high-frequency dielectric constant is $\epsilon_\infty^c = 3.7$ for ZnO (we consider in the following exclusively motions along the c axis of ZnO). The factor 2 stands for the spin of the electrons, e_0 is the elementary charge, and V is the volume of the crystal. In general, the free-electron distribution $f(\vec{k})$ is a cycle-averaged nonequilibrium distribution. $1/m_{\mathrm{eff}}^c(\vec{k})$ is the zz component of the inverse effective mass tensor with the nonparabolic k dependence of the conduction band. The momentum relaxation rate $\gamma_m(\vec{k})$ depends on both the individual k vector of the electron and the entire (non)equilibrium distribution $f(\vec{k})$. In the following, we consider a common momentum relaxation rate for all electrons. A sort of absorption spectrum of the bulk plasmon is given by $\mathrm{Im}[1/\epsilon_c(\omega)]$ with the plasmon resonance (plasma

frequency) determined by the zero point of the real part $\mathrm{Re}[\epsilon_c(\omega)] = 0$ at $\hbar\omega_p = 360$ meV.

Intraband excitation of electrons by the pump pulse at a constant total electron density represents the key interaction to account for the bulk plasmon dynamics. At the very high electron concentration in the ZnO layers, the initial nonequilibrium electron distribution thermalizes into a hot Fermi distribution within the time resolution of the experiment [20]. The Fermi distribution characterized by a high plasma temperature [red curve in Fig. 3(c)] cools back to lattice temperature (300 K) by emission of LO phonons and—at a later stage—of acoustic phonons. To model the temporal evolution of plasma temperature, we performed theoretical calculations, the details of which are described in the Supplemental Material [21]. In short, we describe electron-electron and electron-LO phonon scattering using the loss-function concept including full dynamical screening of the plasma-LO phonon system. For our pumping conditions we calculate the heating and cooling kinetics of the electron plasma as shown in Fig. 2(d). Because of the strongly polar nature of ZnO, a large amount of energy is transferred from the plasma to the lattice during the pump pulse already, followed by a fast cooling down from $T_C \simeq 3500$ to 1000 K within 300 fs. A significant lower cooling rate is observed for $T_C(t) < 1000$ K, due to strong screening of the electron-LO phonon interaction for $0.3 < t < 2$ ps. It is important to note that the changes of plasmon absorption shown in Fig. 2(a) occur on the same time scale as carrier cooling.

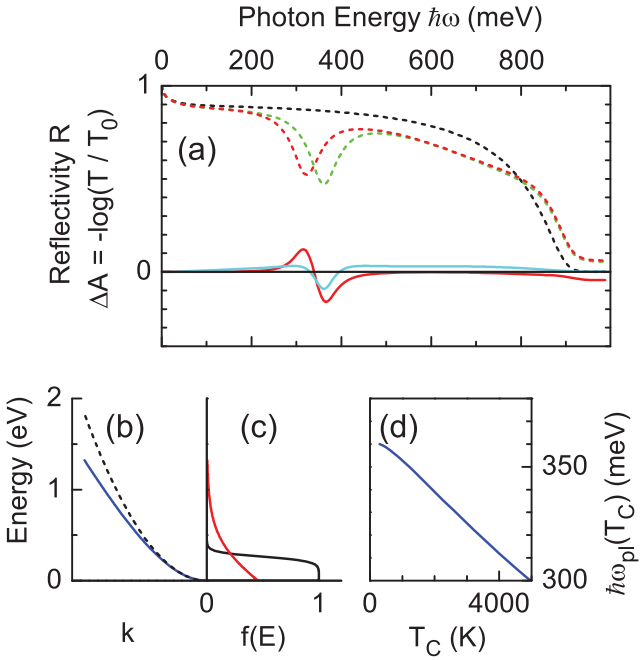

FIG. 3 (color). (a) Black, calculated reflectivity spectrum $R(\hbar\omega)$ of bulk Ga-doped ZnO with an electron concentration of $N_e = 6 \times 10^{20}$ cm^{-3}; green, $R(\hbar\omega)$ of the sample with the additional 100 nm thick ZnO layer [$N_e = 1 \times 10^{20}$ cm^{-3}, structure in Fig. 1(a)] showing clearly its plasmon resonance at $\hbar\omega_p(300\ \mathrm{K}) = 360$ meV; red dashed line, $R(\hbar\omega)$ for a heated electron gas, i.e., $\hbar\omega_p(3500\ \mathrm{K}) = 320$ meV. The corresponding absorbance change $\Delta A = -\log(T/T_0)$ (red solid line) shows the signature of a redshifted plasmon, whereas an increase of its linewidth resulted in the blue ΔA curve. (b) Blue, nonparabolic band structure of ZnO at the conduction band minimum (dashed line, parabolic approximation). (c) Cold (black line, 300 K) and hot (red line, 3500 K) Fermi distributions for $N_e = 1 \times 10^{20}$ cm^{-3}. (d) Calculated plasma frequency $\omega_p(T_C)$ as a function of the carrier temperature T_C.

A hot Fermi distribution [red curve in Fig. 3(c)] in the nonparabolic conduction band of ZnO [blue curve in Fig. 3(b)] results in an increase of the ensemble-averaged zz component of the effective mass tensor to be implemented in Eq. (2). In Fig. 3(d) we show the resulting plasma frequency $\omega_p(T_C)$ as a function of carrier temperature T_C. Heating the electron plasma to $T_C = 3500$ K leads to a 20% reduction of $\omega_p^2(T_C) = 0.8\omega_p^2(300\ \mathrm{K})$, i.e., a redshift of the plasmon resonance. Using Eq. (2) and the Fresnel equations for the full multilayer structure [Fig. 1(a)], we derive the reflectivity spectra shown in Fig. 3(a). $R(\hbar\omega)$ of bulk ZnO with an electron concentration of $N_e = 6 \times 10^{20}$ cm^{-3} is shown as a black dashed line. The green curve displays $R(\hbar\omega)$ of our sample with the additional top layer ($N_e = 1 \times 10^{20}$ cm^{-3}) displaying a bulk plasmon at $\hbar\omega_p = 360$ meV [29]. The red dashed line corresponds to $R(\hbar\omega)$ for an electron gas heated to 3500 K, i.e., $\omega_p(3500\ \mathrm{K}) = 320$ meV. The solid lines show the corresponding absorbance changes ΔA with the red line exhibiting the signature of a redshifted plasmon, in agreement with our experiments. In contrast, an increase of the plasmon linewidth results in the blue ΔA curve.

To account for the time-resolved pump-probe data, we formulated the equations of motion of a harmonic oscillator having both the frequency and oscillator strength of the corresponding time-dependent plasmon [21]. Ultrashort probe pulses with different delays to the pump pulse are used to calculate the field emitted by the plasma current $E(t,\tau)$ in the low-doped ZnO layer as a function of real time t and delay time τ. Finally, a Fourier transform of $E(t,\tau)$ along t gives the spectrally resolved pump-probe signals as shown in Figs. 1(e) and 1(f). Transient absorption changes calculated at fixed probe photon energies for an incident pump energy of 1.8 μJ are shown in Fig. 2(a) (symbols) together with the data (lines). The excellent agreement of our (fitting-parameter-free) theory with the experiment confirms the plasmon redshift due to a transient increase of the average conduction band mass as the predominant mechanism behind the nonlinear response of the bulk plasmon.

Other mechanisms, such as the nonlinear modification of ϵ_∞^c via the (nonresonant) optical Kerr effect by $\Delta\epsilon_\infty^c \approx 10^{-4}$ [30,31] and/or changes of the plasmon line shape by a limited change of the momentum relaxation rate γ_m

[32–35], cannot account for the amplitude and/or spectrally dispersive shape of the pump-probe signals. A change of the sample volume V by the deposition of excess energy from the pump pulse requires acoustic phonon propagation with the sound velocity of ZnO along the c axis of $v_s = 6100$ m/s. This results in an acoustic round-trip time in the 100 nm thick layer of 33 ps, much slower than the transients in Fig. 2.

In conclusion, we studied the nonlinear response of longitudinal bulk plasmons in a highly doped ZnO layer structure, applying a judiciously designed interaction geometry. Two-color femtosecond pump-probe experiments demonstrate a pronounced nonlinear plasmon response, manifested in a femtosecond plasmon redshift and followed by a broadening of the resonance up to ≈2 ps. The experimentally observed redshift is caused by an increase of the average effective electron mass in the strongly heated distribution of conduction band electrons. The strong transient nonlinearity of the layered ZnO system in which the spectral position of the plasmon can be tailored via the electron density holds strong potential for a wide range of applications in ultrafast plasmonics.

We acknowledge financial support by the Deutsche Forschungsgemeinschaft through the Collaborative Research Center 951.

*Deceased.
†woerner@mbi-berlin.de

[1] D. Pines and Ph. Nozieres, *The Theory of Quantum Liquids* (Benjamin, New York, 1966).
[2] A. V. Zayats, I. I. Smolyaninov, and A. A. Maradudin, Phys. Rep. **408**, 131 (2005).
[3] M. I. Stockman, Opt. Express **19**, 22029 (2011).
[4] M. Kauranen and A. V. Zayats, Nat. Photonics **6**, 737 (2012).
[5] W. L. Barnes, A. Dereux, and T. W. Ebbesen, Nature (London) **424**, 824 (2003).
[6] L. Novotny, R. X. Bian, and X. S. Xie, Phys. Rev. Lett. **79**, 645 (1997).
[7] E. Kretschmann, Z. Phys. **241**, 313 (1971).
[8] E. Batke, D. Heitmann, and C. W. Tu, Phys. Rev. B **34**, 6951 (1986).
[9] C. Ropers, C. C. Neacsu, T. Elsaesser, M. Albrecht, M. B. Raschke, and C. Lienau, Nano Lett. **7**, 2784 (2007).
[10] S. Sadofev, S. Kalusniak, P. Schäfer, and F. Henneberger, Appl. Phys. Lett. **102**, 181905 (2013).
[11] S. Kalusniak, S. Sadofev, and F. Henneberger, Phys. Rev. Lett. **112**, 137401 (2014).
[12] P. Halevi, Phys. Rev. B **12**, 4032 (1975).
[13] L. Marton, J. A. Simpson, H. A. Fowler, and N. Swanson, Phys. Rev. **126**, 182 (1962).
[14] D. W. Berreman, Phys. Rev. **130**, 2193 (1963).
[15] S. Campione, I. Brener, and F. Marquier, Phys. Rev. B **91**, 121408(R) (2015).
[16] Equation (1) is valid for $t > 0$, i.e., in the time range of strictly sequential pump-probe interaction. A detailed discussion concerning the influence of the probe spectrum on the nonlinear signal for $t \leq 0$ can be found in W. T. Pollard, S. L. Dexheimer, Q. Wang, L. A. Peteanu, C. V. Shank, and R. A. Mathies, J. Phys. Chem. **96**, 6147 (1992).
[17] R. A. Kaindl, M. Wurm, K. Reimann, P. Hamm, A. M. Weiner, and M. Woerner, J. Opt. Soc. Am. B **17**, 2086 (2000).
[18] B. H. Bairamov, A. Heinrich, G. Irmer, V. V. Toporov, and E. Ziegler, Phys. Status Solidi B **119**, 227 (1983).
[19] Z. Wang, K. Reimann, M. Woerner, T. Elsaesser, D. Hofstetter, J. Hwang, W. J. Schaff, and L. F. Eastman, Phys. Rev. Lett. **94**, 037403 (2005).
[20] T. Elsaesser, J. Shah, L. Rota, and P. Lugli, Phys. Rev. Lett. **66**, 1757 (1991).
[21] See Supplemental Material at http://link.aps.org/supplemental/10.1103/PhysRevLett.115.147401, which includes Refs. [22–28], for calculations of electron dynamics and the resulting changes of plasmon absorption.
[22] B.-C. Shih, Y. Xue, P. Zhang, M. L. Cohen, and S. G. Louie, Phys. Rev. Lett. **105**, 146401 (2010).
[23] E. O. Kane, J. Phys. Chem. Solids **12**, 181 (1960).
[24] M. Woerner and T. Elsaesser, Phys. Rev. B **51**, 17490 (1995).
[25] P. Bowlan, W. Kuehn, K. Reimann, M. Woerner, T. Elsaesser, R. Hey, and C. Flytzanis, Phys. Rev. B **85**, 165206 (2012).
[26] K. Seeger, *Semiconductor Physics*, 5th ed. (Springer, Berlin, 1991).
[27] M. Woerner, T. Elsaesser, and W. Kaiser, Phys. Rev. B **45**, 8378 (1992).
[28] I. Waldmüller, J. Förstner, S. C. Lee, A. Knorr, M. Woerner, K. Reimann, R. A. Kaindl, T. Elsaesser, R. Hey, and K. H. Ploog, Phys. Rev. B **69**, 205307 (2004).
[29] Calculations using Fresnel equations for the full geometry show that in the limit of both an almost vanishing thickness of the top layer ($d \ll \lambda$) and an ideal "metallic" mirror underneath, our layer geometry shows an optical absorption band of the bulk plasmon being exactly proportional to the absorptive $\mathrm{Im}[1/\epsilon(\omega)]$, which is by definition the absorption spectrum of the bulk plasmon and is typically measured in electron loss spectroscopy [13]. For a finite layer thickness and "real" metallic mirrors underneath the dispersive real part $\mathrm{Re}[1/\epsilon(\omega)]$ starts to influence the absorption line shape of the bulk plasmon.
[30] R. Adair, L. L. Chase, and S. A. Payne, Phys. Rev. B **39**, 3337 (1989).
[31] E. Sermuksnis, J. Liberis, M. Ramonas, A. Matulionis, M. Toporkov, H. Y. Liu, V. Avrutin, Ü. Özgür, and H. Morkoç, J. Appl. Phys. **117**, 065704 (2015).
[32] J. H. Hodak, I. Martini, and G. V. Hartland, J. Chem. Phys. **108**, 9210 (1998).
[33] S. Link and M. A. El-Sayed, J. Phys. Chem. B **103**, 8410 (1999).
[34] H. Inouye, K. Tanaka, I. Tanahashi, and K. Hirao, Phys. Rev. B **57**, 11334 (1998).
[35] M. Perner, P. Bost, U. Lemmer, G. von Plessen, J. Feldmann, U. Becker, M. Mennig, M. Schmitt, and H. Schmidt, Phys. Rev. Lett. **78**, 2192 (1997).